Effect of motion discontinuities on discrimination of periodic trajectories

Hugh R. Wilson

Centre for Vision Research, York University, Toronto, Ontario, Canada

Jeffrey Fung

Centre for Vision Research, York University, Toronto, Ontario, Canada

Many biologically important motions are described by periodic trajectories. Radial frequency (RF) trajectories are one example, in which the motion of a difference of Gaussians (DOG) target moves along a path described by a sinusoidal deviation of the radius from a perfect circle (Or, Thabet, Wilkinson, & Wilson, 2011). Here we explore the hypothesis that visual processing of RF trajectories involves global spatio-temporal processes that are disrupted by motion discontinuity. To test this hypothesis, RF trajectories were used that interspersed smooth, continuous motion with three or four discontinuous jumps to other portions of the trajectory. These jumps were arranged so that the entire trajectory was traversed in the same amount of time as in the continuous motion control condition. The motion discontinuities increased thresholds by a factor of approximately 2.1 relative to continuous motion. This result provides support for global spatio-temporal processing of RF motion trajectories. Comparison with previous results suggests that motion discontinuities erase memory for earlier parts of the trajectory, thereby causing thresholds to be based on only the final segment viewed. Finally, it is shown that RF trajectories obey the 1/3 power law characteristic of biological motion.

Introduction

Periodic, smooth motion trajectories are an integral part of biological motion, a typical example being the motion described by each foot in body-centered coordinates during walking or running. In an attempt to elucidate visual analysis of such periodic trajectories, we recently introduced radial frequency (RF) trajectories, in which a moving target traverses a path defined by a sinusoidal deviation of path radius from perfect circular motion (Or et al., 2011). These RF trajectories are the motion analog of spatial RF shapes (Wilkinson, Wilson, & Habak, 1998), which have been helpful in studying intermediate levels of form vision (Loffler, 2008; Loffler, Wilson, & Wilkinson, 2003). Thresholds for RF trajectories have been shown to decrease with the number of sinusoidal cycles at roughly the same rate as in RF patterns, except that trajectory thresholds are universally higher by a factor of about 6.0 (Or et al., 2011). This decreased sensitivity to trajectories relative to static patterns may be a result of imperfect memory for pattern location over the history of movement along a trajectory.

Suprathreshold aspects of RF trajectories have also been explored by measuring increment threshold functions for trajectory discrimination as a function of various amplitude deviations from circular motion. This study provided clear evidence that RF motion discrimination was significantly better at approximately 2.5 times the threshold amplitude than it was either at threshold or at higher multiples of threshold amplitude. (Daar, Or, & Wilson, 2012). Thus, the increment threshold function looks rather like a dipper for water or the Big Dipper constellation. As dipper functions have frequently been interpreted as evidence for a threshold-type nonlinearity (Nachmias & Sansbury, 1974), this suggests that dedicated neural populations may be devoted to processing deviations from circular motion. fMRI studies of RF trajectories provide evidence that they are analyzed in V2, V3, MT, and also posterior parietal and premotor areas (Gorbet, Wilkinson, & Wilson, 2012, 2014).

If there are indeed neural populations dedicated to analyzing deviations from circular periodic trajectories, these populations would have to process a significant range of motion along the trajectory in order to determine whether trajectory curvature varies as a function of location. This raises the question whether RF trajectories are processed as a whole, i.e., globally. Initial evidence from experiments measuring thresholds as a function of number of cycles presented showed that performance improvements were significantly

Citation: Wilson, H. R., & Fung, J. (2015). Effect of motion discontinuities on discrimination of periodic trajectories. *Journal of Vision*, *16*(3):24, 1–8, doi:10.1167/16.3.24.

doi: 10.1167/16.3.24 Received August 19, 2015; published February 18, 2016 ISSN 1534-7362

greater than would be predicted by probability summation (Or et al., 2011). Similar data have previously been obtained supporting global processing of static RF patterns (Bell & Badcock, 2008; Dickinson, McGinty, Webster, & Badcock, 2012; Loffler et al., 2003). In the present paper we sought to further explore global processing of RF trajectory motion by disrupting the continuity of trajectories at specific locations. This represents a motion analog of the disruption of static RF patterns by breaking the contour and jittering the average positions of its parts, a manipulation that has provided strong evidence for global RF processing (Loffler et al., 2003). Our data show that the introduction of motion discontinuities significantly raises thresholds for RF trajectory discrimination, thus providing further evidence for global spatio-temporal processing of periodic motion.

Methods

Apparatus

All stimuli were presented on a VIEWPixx monitor (VPixx Technologies, Quebec, Canada) with spatial resolution of 1920 × 1080 pixels operating at 120 frames/s. At the viewing distance of 127 cm, each pixel subtended 44.0 arcseconds. Calibration of this 10 bit/pixel display revealed a linear correlation of 0.9996 at a mean luminance of 50 cd/m^2. All experiments were conducted using VPixx software running on an Apple iMac computer (Apple, Cupertino, CA).

Stimuli

The moving pattern in all experiments was a concentric difference of Gaussians (DOG) defined as a function of radius R relative to its center by:

$$\mathrm{DOG}(R) = 1.8\exp\left(-\frac{R^2}{\sigma^2}\right) - 0.8\exp\left(-\frac{R^2}{(1.5\sigma)^2}\right) \quad (1)$$

The space constant σ was set to 7.1 arc min, making the peak spatial frequency 2.17 cpd and the bandwidth 1.79 octaves at half amplitude. The DOG mean luminance was identical to that of the screen, and the contrast was 100%.

Radial frequency (RF) trajectories are defined by the equation:

$$r(vt) = r_0\left(1 + A\sin(\omega vt + \phi)\right) \quad (2)$$

where r is the radius of the trajectory as a function of velocity v and time t. Note that r and r_0 refer to the radius of the RF trajectory relative to the center of the screen, while R refers to the radius of the target only. Amplitude A of the deviation from circularity was varied to determine the threshold for RF trajectory discrimination, with $A = 0.0$ corresponding to a circle of radius r_0. Finally, the radial frequency of the trajectory is given by an integer value of ω, and the phase by ϕ. Two radial frequencies were used in these experiments: $\omega = 3$ cycles, and $\omega = 4$ cycles, and these will be referred to as RF3 and RF4 trajectories respectively. The base radius $r_0 = 1.0°$ in all but one experiment (documented in the following material). Examples are depicted in Figure 1, where the arrows show that motion was always in clockwise direction. The velocity v was either 6.28°/s (1.0 s transit time around the trajectory) or 12.56°/s (0.5 s transit time). Note that these are average velocities (strictly speeds), as speed varied slightly for RF trajectories and only remained constant for the circular pattern. Previous work has shown that keeping the speed strictly constant (by varying the angular velocity appropriately) does not affect threshold measurements (Or et al., 2011).

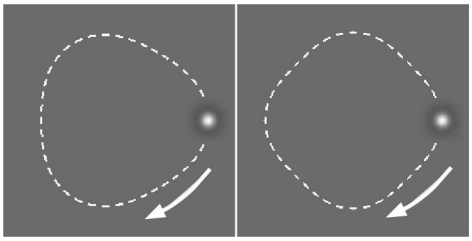

Figure 1. Examples of RF3 (left) and RF4 (right) trajectories. The DOG stimulus moved in a clockwise direction (arrows) once around the trajectory indicated by the dashed lines. The dashed lines and arrows are for illustration only and were not present in the experiments.

Compared to continuous movement along RF trajectories described by Equation 2, the major manipulation to test the global processing hypothesis was to introduce one discontinuous jump per RF cycle into the stimulus motion. This is illustrated in Figure 2. Consider the RF3 trajectory depicted in 2C. In this instance the target appeared at the far right arrowhead and moved continuously along the trajectory segment labeled 1 in a clockwise direction. The target then jumped to the segment labeled 2 and again moved clockwise. Finally, the target jumped to segment 3 to complete its clockwise traverse of the RF3 trajectory. In this instance, the points of motion discontinuity occurred at the radius maxima. Figure 2D illustrates the same RF3 trajectory but with the discontinuities occurring at the loci of minimum radius. Figure 2A and B show the same manipulations for an RF4 trajectory, which contains one additional discontinuity due to the increased number of RF cycles. Note that in all four cases the DOG target occupies the same set of positions

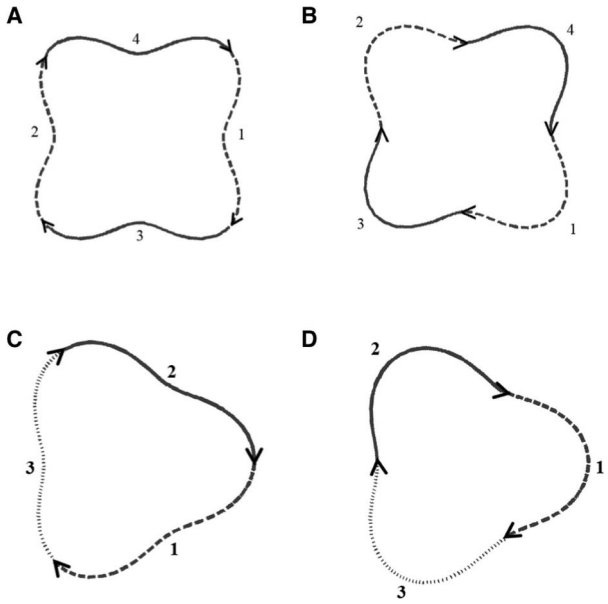

Figure 2. Examples of the four types of discontinuous trajectories used in the experiments. A and B depict RF4 discontinuous trajectories, while C and D depict RF3 trajectories. In C, for example, the DOG target first moved along dashed trajectory segment #1, then jumped to the beginning of solid trajectory segment #2 and moved along it. Finally, it jumped to dotted trajectory segment #3 to complete the trajectory motion. Segment numbering indicates motion sequence in all four diagrams. A and C describe the Max Jump condition, while B and D describe the Min Jump condition.

around the trajectory as in the continuous case. The only difference from the continuous case is the presence of three or four jumps. The comparison circular trajectories were also discontinuous at the same locations and times as the RF trajectories to preclude motion discontinuities providing a trivial basis for discrimination.

Procedure

Observers initiated each trial with a button press. Following this, either a circular or RF trajectory was presented for sufficient time to complete one cycle. There was then a 1-s pause before the second trajectory was presented. The observer's task was to indicate with a button press the interval in which they believed the RF trajectory had been presented. Discrimination thresholds were measured using a staircase procedure in which three correct responses resulted in a decrease in amplitude to make the task harder, while one incorrect response produced an amplitude increase. The last eight reversals were averaged, which produces an estimate of the 79% correct discrimination threshold when using the three correct versus one incorrect

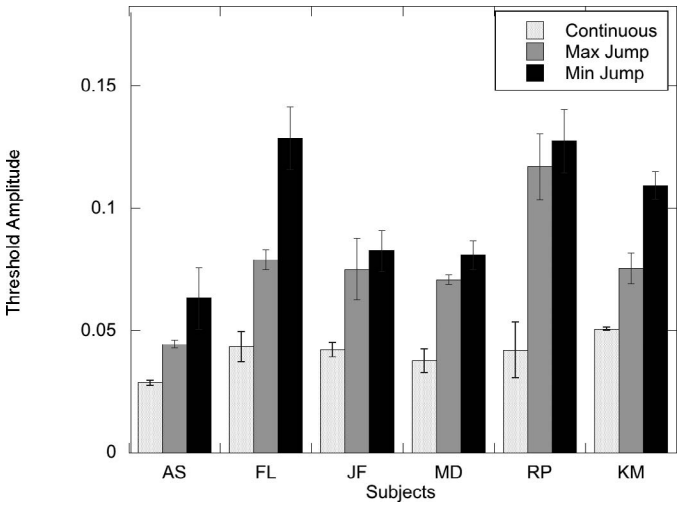

Figure 3. Data comparing continuous motion with Max and Min Jump conditions for RF4 trajectories and six subjects. Error bars in this and all subsequent Figures indicate standard errors of the mean. Both Max and Min Jump conditions produced significant threshold elevations relative to continuous motion.

procedure (Garcia-Pérez, 1998; Wetherill & Levitt, 1965) In each experiment measurements were made for a single RF trajectory (three or four cycles in different experiments), and the continuous and discontinuous motion examples were also measured in different experiments.

A total of eight females and nine males participated in these experiments, including one of the authors (JF). Their mean age was 22.8 ± 4.2 years, and all had normal or corrected-to-normal vision. Either five, six, or seven observers completed each different experimental condition.

Results

The first experiment compared discrimination of RF4 trajectories from circles under three different experimental conditions: continuous motion, jumps at maximum radius (Max Jump), and jumps at minimum radius (Min Jump). In each case the comparison circular trajectory contained jumps at the same locations and times as the RF4 trajectory. Results for six subjects with standard error bars are shown in Figure 3, where thresholds are values of amplitude A in Equation 2. It is quite obvious that the jump conditions (dark gray and black) significantly elevated thresholds relative to continuous motion (light gray). Threshold averaged 0.041 ± 0.003 for Continuous, 0.077 ± 0.009 for Max Jump, and 0.099 ± 0.011 for Min Jump. A one-way, repeated-measures ANOVA showed a significant effect of motion trajectory type, $F(2, 10) = 25.75$, $p < 0.0002$. Subsequent t tests with Bonferroni

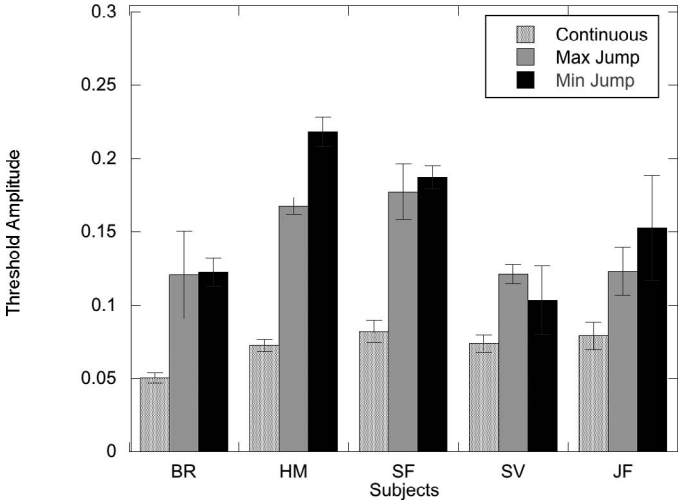

Figure 4. Data for five subjects comparing Jump conditions with continuous motion for RF3 trajectories. Both Jump conditions again produced significant threshold elevations relative to continuous motion.

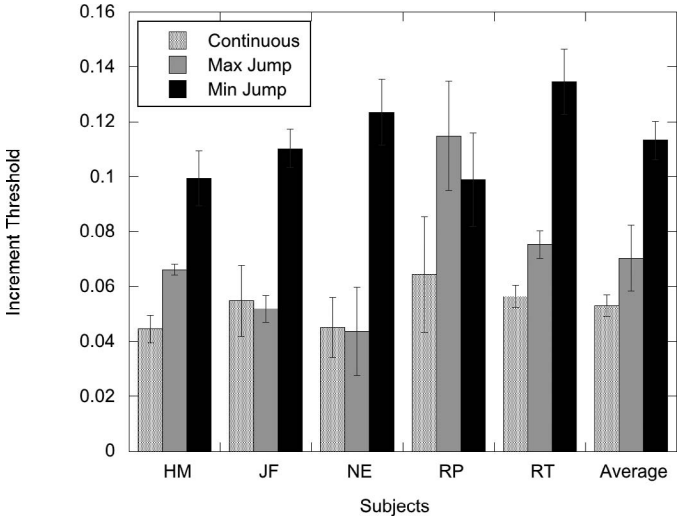

Figure 5. Suprathreshold discrimination for RF4 trajectories at four times mean detection threshold. Data for five subjects plus averages across subjects are shown. Only the Min Jump condition produced a statistically significant threshold elevation relative to continuous motion. Max Jump produced a trend in the same direction but was not significant.

correction showed that thresholds for both Jump conditions were significantly greater than the Continuous trajectory threshold, but there was no significant difference between the Max Jump and Min Jump conditions.

A comparable experiment used RF3 trajectories to determine whether these results generalized across radial frequencies. Results for five subjects are plotted in Figure 4. Means for the three conditions were: Continuous 0.072 ± 0.006; Max Jump 0.142 ± 0.013; Min Jump 0.157 ± 0.021. A one-way, repeated-measures ANOVA again revealed a significant effect of trajectory type, $F(2, 8) = 19.59$, $p < 0.0008$. Pairwise t tests with Bonferroni correction again revealed that both jump conditions produced significantly higher thresholds than the continuous condition, but there was no statistically significant difference between Max Jump and Min Jump.

Thus, trajectory discrimination is disrupted for both RF3 and RF4 by the introduction of discontinuous jumps, and the threshold elevations (average of Max and Min Jumps divided by Continuous) that jumps produced in the two conditions were virtually identical: 2.08 ± 0.022 for RF3 versus 2.15 ± 0.013 for RF4. However, the Max Jump and Min Jump conditions did not produce significantly different threshold elevations. As a final point here, it may also be noted that the thresholds were higher for RF3 than for RF4 trajectories under both Continuous and Jump conditions. This is in agreement with previous RF trajectory measurements for continuous motion (Or et al., 2011).

The measurements just described represent thresholds for discriminating RF trajectories from circular trajectories. So, we wondered whether the same pattern would hold for suprathreshold discrimination between RF trajectories with different amplitudes. Accordingly, an RF4 trajectory with base amplitude of 4.0 times the previously measured mean detection threshold was discriminated from RF4 trajectories with progressively higher amplitudes in order to measure the increment threshold. The same staircase procedure described above was used to estimate the 79% correct discrimination point. Figure 5 shows data for five observers plus averages for each of the three motion conditions. A repeated-measures ANOVA revealed a highly significant effect of trajectory type, $F(2, 8) = 13.36$, $p < 0.003$. Pairwise t tests showed that thresholds for the Min Jump condition were significantly greater than those for either the continuous or Max Jump conditions, $t(8) = 5.02$, $p < 0.001$; $t(8) = 3.56$, $p < 0.008$ respectively. However, there was no significant difference between the Max Jump and continuous conditions, $t(8) = 1.44$, $p = 0.19$. Thus, only the Min Jump condition significantly elevated thresholds under these suprathreshold conditions, although there was an insignificant trend in the same direction for the Max Jump condition.

These increment threshold measurements were repeated at 4.0 times threshold for the RF3 trajectories, and results for six observers are plotted in Figure 6. Statistical analysis using repeated-measures ANOVA showed a significant effect of trajectory type, $F(2, 10) = 5.59$, $p < 0.024$. Subsequent t tests revealed that only the Min Jump condition was significantly larger than the continuous condition, $t(10) = 3.32$, $p < 0.008$, although the Max Jump versus continuous condition approached significance, $t(10) = 1.97$, $p = 0.077$. Max

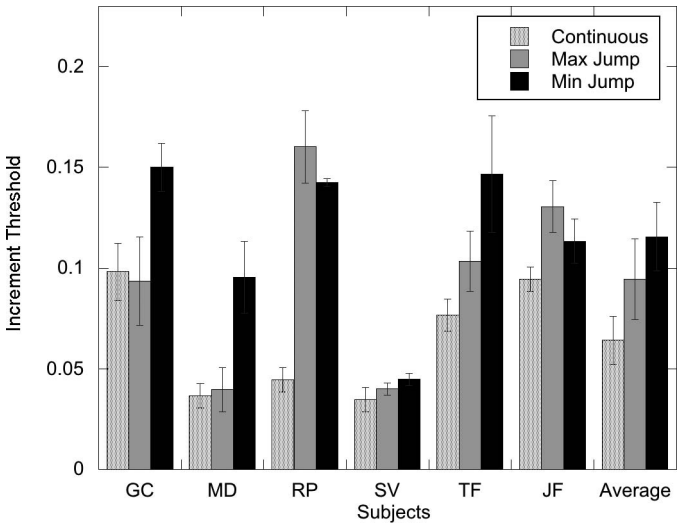

Figure 6. Suprathreshold discrimination for RF3 trajectories. Data are shown for six subjects plus the averages. Only the Min Jump condition produced a significant threshold elevation relative to continuous motion.

Jump versus Min Jump thresholds were not significantly different, $p(10) = 1.35$, $p = 0.21$. Thus, the same pattern of results for suprathreshold increment thresholds was apparent for both RF3 and RF4 trajectories.

All data so far have been obtained at a mean target speed of 6.28°/s and a mean radius $r_0 = 1.0°$. As a control experiment to determine whether these variables were critical to our results, thresholds for discrimination between circular trajectories and RF4 or RF3 trajectories were repeated under two further

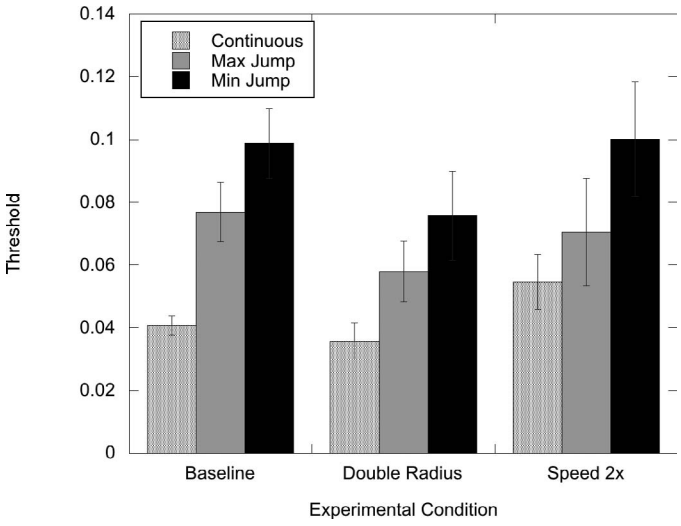

Figure 7. Effects of target speed and mean radius on RF4 trajectory discrimination. Data are means for six subjects. There was no significant effect of speed. However, both Jump conditions produced statistically significant threshold elevations, and Min Jump also produced a larger elevation than Max Jump.

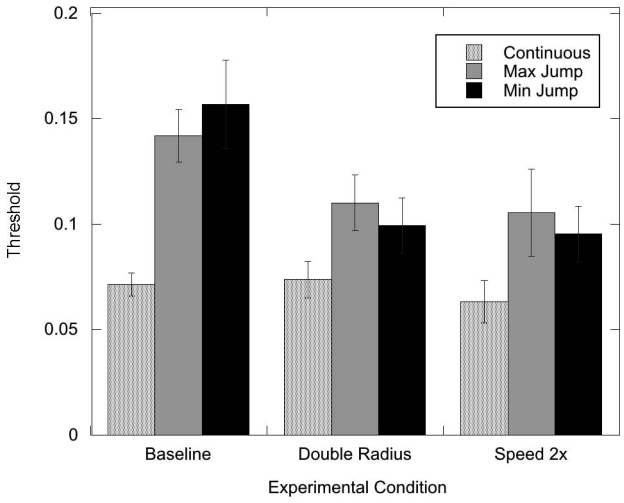

Figure 8. RF3 trajectory discrimination effects of speed and radius. Results are means across five observers. Threshold elevations for the Jump conditions were significant as expected from the previous results. However, there was also a significant effect of speed.

conditions. In the Double Radius condition, $r_0 = 2.0°$, and target speed was also doubled to 12.56°/s. In the Speed 2× condition, only the speed was doubled to 12.56°/s, while the radius remained at 1.0°. Results for six subjects tested with RF4 trajectories are graphed in Figure 7. The baseline condition replots the means for these subjects from Figure 3. A two-way ANOVA with Jump condition and Speed as factors showed a significant effect of Jump condition, $F(2, 45) = 12.37$, $p < 0.0001$, but no effect of Speed, $F(2, 45) = 2.17$, $p = 0.126$. In addition, there was no interaction between conditions, $F(4, 45) = 0.274$, $p = 0.894$. Pairwise comparisons of the three Jump conditions revealed that all three comparisons were statistically significant at the $p < 0.02$ level.

Repeating this speed variation experiment using RF3 trajectories produced the data plotted in Figure 8. The baseline data represent means for the five observers obtained from the data in Figure 4. A two-way ANOVA this time revealed significant effects of both the Jump condition, $F(2, 36) = 12.23$, $p < 0.0001$, and the Speed condition, $F(2, 36) = 5.50$, $p < 0.01$. There was no interaction, $F(4, 36) = 1.39$, $p = 0.258$. The effect of jump condition was expected and was consistent with all previous data. However, the significant Speed effect here was not expected given the results with RF4 trajectories in Figure 7 above. Subsequent pairwise t tests showed that the Baseline versus Double Radius and Baseline versus Speed 2× were both significant, $t(36) = 2.55$, $p < 0.02$, and $t(36) = 3.11$, $p < 0.005$ respectively. However, there was no significant difference between Double Radius and Speed 2×, $t(36) = 0.56$, $p = 0.577$. From Figure 8 it seems apparent that these results are due to the smaller disruptions

produced by the Max Jump and Min Jump conditions in the Double Radius and Speed 2× conditions relative to baseline.

Discussion

Our goal was to determine whether a small number of motion discontinuities would raise thresholds for trajectory discrimination. For both RF3 and RF4 trajectories, threshold elevations averaging 2.11 were obtained. Furthermore, there was no statistically significant difference between the Max Jump and Min Jump condition at either radial frequency. To see whether these results also held for suprathreshold RF trajectories that were clearly discriminable from circles, increment thresholds were measured at four times the threshold trajectory amplitude. The results showed that for both RF3 and RF4 trajectories the jump condition significantly raised increment thresholds relative to continuous motion. However, in both cases subsequent pairwise tests showed that these threshold elevations were due to the Min Jump condition, and that the Max Jump condition trended in the same direction but did not reach statistical significance.

As the Max Jump and Min Jump conditions produced similar elevations when discriminated from a circle, it suggests that the visual system uses trajectory information in the regions of the Max and Min locations to compute trajectory shape. Although integration of information at all points around the RF trajectory is also possible, the Max and Min positions are the loci at which the curvature is most different from that of the circle. This agrees with previous work in which thresholds were measured for 0.5 cycle of an RF3 either centered on the max or min point. Both conditions elevated thresholds to the same degree (Or et al., 2011). In comparison, as only the Min Jump condition produced a significant threshold elevation under suprathreshold conditions, it would appear that trajectory shape information at the minimum amplitude points is most important for discrimination significantly above threshold. Further studies should help to elucidate this.

As the main experiments had all been conducted with a target speed of 6.28°/s in visual angle, we also repeated the experiments at double the speed to determine whether this might alter the results. In this case different results were found for RF3 and RF4 trajectories, although in both cases the Jump conditions significantly increased thresholds relative to the continuous motion condition. The speed manipulation was statistically significant for the RF3 trajectories but not for the RF4 trajectories. An examination of Figure 8 indicates that in the RF3 condition the speed manipulations did not affect continuous motion, but increased speed did improve the thresholds for the two Jump conditions. It is difficult to suggest an obvious explanation for this result, so it must await further experimentation. Certainly one possibility is that increasing speed only enhances performance at very low radial frequencies.

The almost ubiquitous threshold elevation produced by only three or four points of motion discontinuity provides evidence for global processing of periodic motion trajectories. It is clear that the brain must use short-term memory to store the spatio-temporal trajectory along which the target had moved. This would convert trajectory shape analysis into a spatial pattern analysis task with the added complexity of some blurring resulting from imperfect memory storage (memory decay) during the course of the motion. Indeed, RF trajectory thresholds are higher than thresholds for static RF shapes by a factor of up to 6.0 (Or et al., 2011), and this might be explained through memory decay.

Such a trajectory memory model also suggests a quantitative explanation of threshold elevations due to motion discontinuities. Suppose that each sudden jump causes an active erasure of previous continuous motion memory. This would force the observer to base discrimination on only the last cycle of motion, i.e., one-third or one-quarter of the entire trajectory. Previously reported thresholds for RF3 trajectories show that the presence of just one cycle rather than three elevates thresholds by a factor of 2.02 (Or et al., 2011). This is statistically indistinguishable from the threshold elevation of 2.1 reported here for RF3. Thus, a memory storage model plus erasure due to jumps is quantitatively consistent with our data and is further evidence for global trajectory processing. It is worth noting here that the magnocellular pathway is suppressed during saccadic eye movements (Burr, Morrone, & Ross, 1994), so it is plausible that target jumps might have an analogous effect on trajectory memory.

Although the motion jump discontinuities employed here are unnatural, there is a related condition in which position jumps do occur: motion behind an occluder. Consider the discontinuous RF3 trajectory shown schematically in Figure 3C. Suppose that this was a continuous motion trajectory, except that the segment labeled 3 went behind an occluder. Then one would observe smooth motion along segment 1 followed by 1/3 s with no visible target, then finally the motion along segment 2. There are of course two differences between this occlusion scenario and the jumps employed in our experiments. First, the occlusion duration is substantial rather than being a single frame shift. Second, only two-thirds of the total trajectory would be visible. However, it seems likely that RF trajectories will be

useful in studying the effects of natural motion occlusion.

We have argued that RF trajectories may be related to biological motion in body-centered coordinates. In related research, there has been much work on the kinematic laws underlying human motion production in tasks like handwriting or random doodling. These studies all point to a power law relating the instantaneous tangential motion velocity V to the local radius of trajectory curvature R (Lacquaniti, Terzuolo, & Viviani, 1983). Specifically:

$$V = k \cdot R^{1/3} \quad (3)$$

where k represents a gain factor. Furthermore, trajectories of a moving dot on a screen perceptually seem most natural and to have the least variation in velocity when this power law is obeyed (Viviani & Stucchi, 1992). As RF trajectories were not specifically designed with this law in mind, it is worth asking whether they are consistent with it. For low amplitudes A in Equation 2, there is little variation from a circle, for which R and V are constant, so these stimuli are certainly consistent with this law. To test relatively large variations in radius of curvature for adherence to this law, analytic formulas for both V and R along an RF trajectory were derived using Symbolic Calculator for OSX (Voxeloid Kft). The result was:

$$V = \left[(A\omega^2 + 2A)\cos(\omega\theta) + A^2(\omega^2 - 1)\sin(\omega\theta) + A^2(\omega^2 + 1) + 1\right]^{1/3} R^{1/3} \quad (4)$$

where θ is angular velocity. Approximating this by a first order Taylor series in θ near $\theta = 0$ yields:

$$V = \left[A^2(\omega^2 + 1) + A(\omega^2 + 2) + 1\right]^{1/3} R^{1/3} \quad (5)$$

This is exactly equivalent to Equation 3 above with the term in brackets representing the value of the constant k as a function of A and ω. Figure 9 shows plots of Equation 5 for $A = 0.5$ and three values of ω compared with the exact results in Equation 4. Clearly, RF trajectory motion precisely replicates the biological motion relationship represented in Equation 3 across a wide range of radial frequencies and amplitudes.

In conclusion, the data reported here provide further evidence for global processing of RF trajectories. As these trajectories are only defined over time, spatio-temporal memory storage must clearly play a role. BOLD activity in response to RF trajectory perception suggests that such storage may involve both posterior parietal and premotor cortex (Gorbet et al., 2014). This makes it tempting to speculate that the mirror neuron system (Fabbri-Destro & Rizzolatti, 2008; Rizzolatti & Sinigaglia, 2010) may be involved in RF trajectory memory. Furthermore, RF trajectories obey the 1/3 power law characteristic of biological motion (Lacquaniti et al., 1983). These observations suggest a number of fruitful directions for future trajectory research.

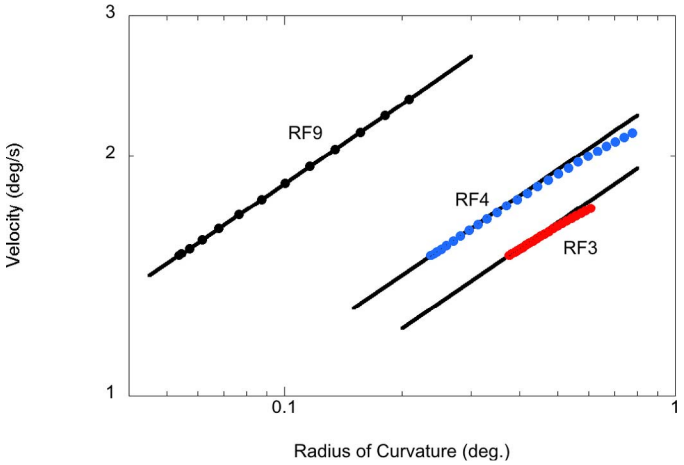

Figure 9. Plot of RF trajectory tangential velocity as a function of Radius of Curvature for RF3 (red), RF4 (blue), and RF9 (black). Amplitude $A = 0.5$ in each case. Dots show the exact theoretical relationship from Equation 4, while solid black lines show the Taylor series approximation in Equation 5. These 1/3 power law fits show an excellent fit to the kinematic data discussed in the text.

Keywords: periodic motion, global processing, motion discontinuity

Acknowledgments

This research was supported in part by NSERC grant #227224 to HRW and NSERC CREATE training grant support for JF. We thank F. Wilkinson for introducing us to the literature on biological motion kinematics exemplified by the 1/3 power law.

Commercial relationships: none.
Corresponding author: Hugh R. Wilson.
Email: Hrwilson@yorku.ca.
Address: Centre for Vision Research, York University, Toronto, Ontario, Canada.

References

Bell, J., & Badcock, D. R. (2008). Luminance and contrast cues are integrated in global shape detection with contours. *Vision Research*, *48*(21), 2336–2344.

Burr, D. C., Morrone, M. C., & Ross, J. (1994). Selective suppression of the magnocellular visual

pathway during saccadic eye movements. *Nature*, *371*, 511–513.

Daar, M., Or, C. F., & Wilson, H. R. (2012). Increment thresholds for radial frequency trajectories produce a dipper function. *Vision Research*, *73*, 46–52.

Dickinson, J. E., McGinty, J., Webster, K. E., & Badcock, D. R. (2012). Further evidence that local cues to shape in RF patterns are integrated globally. *Journal of Vision*, *12*(12):16, 1–17, doi:10.1167/12.12.16. [PubMed] [Article]

Fabbri-Destro, M., & Rizzolatti, G. (2008). Mirror neurons and mirror systems in monkeys and humans. *Physiology*, *23*, 171–179.

Garcia-Pérez, M. A. (1998). Forced-choice staircases with fixed step sizes: Asymptotic and small-sample properties. *Vision Research*, *38*, 1861–1881.

Gorbet, D. J., Wilkinson, F., & Wilson, H. R. (2012). An fMRI examination of the neural processing of periodic motion trajectories. *Journal of Vision*, *12*(11):5, 1–15, doi:10.1167/12.11.5. [PubMed] [Article]

Gorbet, D. J., Wilkinson, F., & Wilson, H. R. (2014). Neural correlates of radial frequency trajectory perception in the human brain. *Journal of Vision*, *14*(1):11, 1–19, doi:10.1167/14.1.11. [PubMed] [Article]

Lacquaniti, F., Terzuolo, C., & Viviani, P. (1983). The law relating the kinematic and figural aspects of drawing movements. *Acta Psychologica*, *54*, 115–130.

Loffler, G. (2008). Perception of contours and shapes: Low and intermediate stage mechanisms. *Vision Research*, *48*, 2106–2127.

Loffler, G., Wilson, H. R., & Wilkinson, F. (2003). Local and global contributions to shape discrimination. *Vision Research*, *43*, 519–530.

Nachmias, J., & Sansbury, R. V. (1974). Grating contrast: discrimination may be better than detection. *Vision Research*, *14*, 1039–1042.

Or, C., Thabet, M., Wilkinson, F., & Wilson, H. R. (2011). Discrimination and identification of periodic motion trajectories. *Journal of Vision*, *11*(8):7, 1–11, doi:10.1167/11.8.7. [PubMed] [Article]

Rizzolatti, G., & Sinigaglia, C. (2010). The functional role of the parieto-frontal mirror circuit: Interpretations and misinterpretations. *Nature Reviews Neuroscience*, *11*, 264–274.

Viviani, P., & Stucchi, N. (1992). Biological movements look uniform: Evidence of motor-perceptual interactions. *Journal of Experimental Psychology: Human Perception and Performance*, *18*, 603–623.

Wetherill, G. B., & Levitt, H. (1965). Sequential estimation of points on a psychometric function. *British Journal of Mathematical and Statistical Psychology*, *18*, 1–10.

Wilkinson, F., Wilson, H. R., & Habak, C. (1998). Detection and recognition of radial frequency patterns. *Vision Research*, *38*, 3555–3568.